

Second-Order Chemical Reactions in a Nonhomogeneous Turbulent Fluid

GEORGE VASSILATOS and H. L. TOOR

Carnegie Institute of Technology, Pittsburgh, Pennsylvania

Very rapid, rapid, and slow second-order reactions were studied in an isothermal turbulent flow reactor. The two aqueous reactant solutions were separately introduced through many alternate jets and the reaction took place in the resulting nonhomogeneous mixture. Very rapid reactions were diffusion controlled and were in agreement with earlier theory. All reactions followed second-order rate laws based on time average quantities. The apparent reaction velocity constant was controlled by the mixing for very rapid reactions, by the chemical kinetics for slow reactions, and by both mechanisms for rapid reactions.

When a homogeneous chemical reaction takes place in a turbulent fluid the local instantaneous rate of reaction can be assumed to be described by the normal laws of homogeneous chemical kinetics. However, the local time average rate of reaction, r_i , the *mean rate*, may be greater than, equal to, or less than the homogeneous rate at the local time average concentration, the *homogeneous mean rate*. Although the above statements are true whether or not the system is isothermal, in this paper only isothermal situations are considered.

For the purposes of this discussion a homogeneous solution or mixture is one in which the RMS concentration fluctuations of all species are zero. The mean rate obviously equals the homogeneous mean rate in homogeneous solutions and this is true even in nonhomogeneous solutions if the reaction is first order.

In nonhomogeneous solutions the mean rate of a type I second-order reaction, $A + A \rightarrow \text{product}$, is greater than the homogeneous mean rate, while the mean rate of a type II second-order reaction, $A + B \rightarrow \text{product}$, may be greater or less than the homogeneous mean rate, depending upon how the reactants are introduced; greater if the reactants are premixed, less if they are not. (The above assertions are easily justified by examining the appropriate time average expressions and noting that premixing gives a positive correlation between the fluctuating reactant concentrations, while lack of premixing gives a negative correlation.)

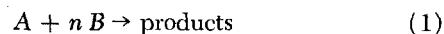
The deviation from the homogeneous mean rate depends upon the rate of the reaction relative to the rate of mixing. Three arbitrary divisions are convenient: very rapid reactions, rapid reactions, and slow reactions. They correspond, respectively, to reaction rates much faster than the rate of mixing, reaction rates of the same order as the rate of mixing, and reaction rates much slower than the rate of mixing. The latter case is the simplest, and most reactor design studies have been concerned with this problem. It is under reasonably good control. [It is noted that in the flow methods of studying *rapid* chemical reactions in solution (14), the reactions are slow in the above sense, since the experiments are designed to make the mixing much faster than the reaction.]

Very rapid and rapid reactions present an entirely different problem, for here the detailed turbulent motion can have a profound effect on the rate of reaction, es-

pecially with type II second-order reactions. Here two molecular species must be brought into intimate contact by molecular diffusion, aided and abetted by the turbulent motion.

A premixed reactor is now an impossibility; the mixer is the reactor and the problem, which is the subject of this study, is to determine the mean rate of reaction, hence the mean conversion, under these conditions.

Irreversible isothermal second-order type II reactions in dilute incompressible solution with stoichiometry given by



and rate law by

$$r_A = -k_r C_A C_B = r_B/n \quad (2)$$

are to be considered.

The transport equations are

$$\frac{\partial C_i}{\partial \theta} + \nabla \cdot V C_i = \nabla \cdot D_i \nabla C_i + r_i, \quad i = A, B \quad (3)$$

and are intractable in this form. The time averaged form is

$$\frac{\partial \bar{C}_i}{\partial \theta} + \nabla \cdot \bar{V} \bar{C}_i = \nabla \cdot (D_i \nabla \bar{C}_i - \bar{V}' C_i') + \bar{r}_i, \quad i = A, B \quad (4)$$

with

$$\bar{r}_A = -k_r (\bar{C}_A \bar{C}_B + \bar{C}_A' \bar{C}_B') = \frac{\bar{r}_B}{n} \quad (5)$$

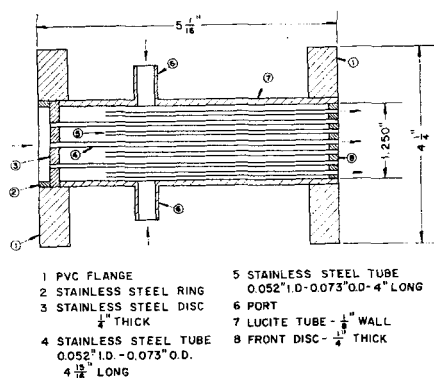


Fig. 1. Mixing device.

George Vassilatos is with E. I. duPont de Nemours and Company, Inc., Wilmington, Delaware.

In order to solve Equations (4) and (5) for $\overline{C_i}$, and hence the mean rate of reaction, the cross product terms $\overline{C_i'V'}$ and $\overline{C_A'C_B'}$ must be evaluated. A reasonable hypothesis for the former would be the usual eddy diffusivity form.

$$-\overline{V'C_i'} = \epsilon \nabla \overline{C_i} \quad (6)$$

However, further information concerning $\overline{C_A'C_B'}$ is still required, for it is the term $\overline{C_A'C_B'}/\overline{C_A}\overline{C_B}$ that sets the difference between the mean and homogeneous mean reaction rates. This term is important for rapid and very rapid reactions where the reactants must be separately fed to the reactor; C_A' and C_B' are then negatively correlated and the mean reaction rate is less than the homogeneous mean rate.

Corrsin (2, 3, 4) has done some preliminary analysis of the first-order and type I second-order reactions using the statistical theory of turbulence, but type II second-order reactions have been analyzed only at the diffusion controlled limit (15).

As k_r increases without limit, $\overline{C_A'C_B'}$ must approach $-\overline{C_A}\overline{C_B}$ in order to keep $\overline{r_A}$ finite. This is the case of very rapid reactions, the diffusion controlled limit; the reaction takes place on reaction surfaces within eddies (15) and the rate of molecular diffusion to these surfaces controls the rate of reaction.

At this limit Toor (15) showed that it is possible to bypass the details of the turbulent motion when $D_A = D_B$ and to obtain a direct relationship between the conversion and mixing from Equations (1), (2), and (3). This analysis was based on the earlier work of Burke and Schumann (1) and Hawthorne, Weddel, and Hottel (7).

Thus, if solvent containing reactant A and solvent containing reactant B meet at $Z = 0$ in a tubular reactor, the fluids intermingle and at some downstream distance Z_0 the mixture approaches uniformity on a coarse scale ($\overline{C_i}$ independent of tube radius) and this can occur before homogeneity is reached. For $Z > Z_0$ the problem is one dimensional and the results are then particularly simple.

If the two streams enter in stoichiometric proportions, the time average fractional conversion of either species measured from Z_0 is given by the simple relationship (15)

$$F(1) = 1 - \Gamma^0/\Gamma^\infty \quad (7)$$

where Γ^0 is the root mean square concentration fluctuation that would exist at any axial distance greater than Z_0 if species 2 were not present; that is, if species 1 did not react but was merely mixed with the solvent in the mixer, and Γ^∞ is the RMS concentration fluctuation at the plane Z_0 .

Thus, Equation (7) indicates a linear relationship between the conversion and the accomplished mixing; this latter quantity depends only upon the turbulent field and measures the ability of the turbulent field to even out concentration fluctuations.

TABLE 1. SYSTEMS USED

Reactants	Reaction velocity constant k_r , l./mole sec., 30°C.	References
HCl-NaOH		
HCl-LiOH		
HOOC-COOH-2LiOH	$\sim 10^{11}$	5
HCOOH-LiOH		
CO ₂ -2NaOH	1.24×10^4	12
CO ₂ -nNH ₃ (n varies from 1 to 2)	5.85×10^2	13, 16, 17, 18
HCOOCH ₃ -NaOH	4.7×10^1	11

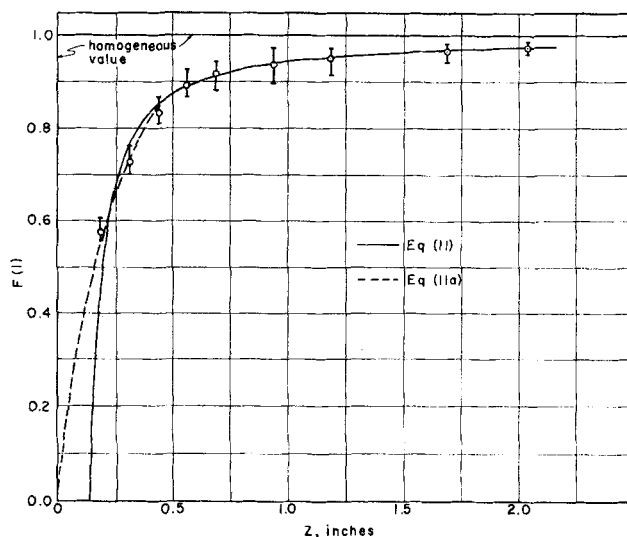


Fig. 2. F vs. Z , $\beta = 1$, very rapid reactions.

For nonstoichiometric mixtures Equation (7) is replaced by (15)

$$F = 1 + (\beta - 1) \left\{ 1 + \frac{\gamma_0 \Gamma_0/\Gamma^\infty}{\sqrt{2}} \operatorname{ierfc} \frac{1}{\sqrt{2} \gamma_0 \Gamma_0/\Gamma^\infty} \right\} \quad (7a)$$

where

$$\frac{\gamma_0}{\sqrt{2}} \operatorname{ierfc} \frac{1}{\sqrt{2} \gamma_0} = \frac{\beta}{1 - \beta} \quad (7b)$$

$$\beta = \frac{\overline{C_{B_0}}}{n \overline{C_{A_0}}} \quad (7c)$$

and F is the conversion of species A, the limiting reactant.

These predictions were confirmed experimentally by Keeler, Petersen, and Prausnitz (8) for flow behind a grid using the very rapid reaction of ammonium hydroxide with acetic acid.

Earlier experiments of this type were carried out by Hawthorne et al. (1), Kramers (9), and Danckwerts (10). In addition there have been a number of limited experiments carried out to determine the distance for mixing in connection with the flow method of studying chemical reactions in solution (14).

This study is concerned with the determination of the mean rate of reaction over the full range of reaction velocities, from very rapid to slow. A convenient means of following the reaction is to determine the temperature change along the reactor (which is generally about $\pm 0.2^\circ\text{C}$. for complete conversion in this work). When the system is uniform on a coarse scale ($Z > Z_0$) Equations (4) and (6) give

$$\bar{u} \frac{d\overline{C_i}}{dZ} = \frac{d}{dZ} (D_i + \epsilon_z) \frac{d\overline{C_i}}{dZ} + \bar{r}_i, \quad i = A, B \quad (8)$$

and for similar conditions with an adiabatic reactor, the energy equation yields

$$\bar{u} \frac{d\overline{T}}{dZ} = \frac{d}{dZ} (\alpha + \epsilon_{hz}) \frac{d\overline{T}}{dZ} + \frac{\bar{r}_A}{\rho C_p} \Delta H \quad (9)$$

The axial eddy diffusivities of heat and mass are taken to be equal and much larger than the molecular values and since the boundary conditions on Equations (8) and (9) are similar, the solutions to the two equations must satisfy the equation

$$\Delta \bar{C}_A = \frac{\rho C_P}{\Delta H} \Delta \bar{T} \quad (10)$$

Hence measurement of the temperature rise gives the conversion, and if in addition ϵ_z and k_r are known, \bar{C}_A/\bar{C}_B may also be determined from Equation (5). In this work the axial diffusion appears to play a small role, so the assumptions concerning these terms are not critical. Equation (10) is also valid in a nonuniform field in which the total diffusivities of heat and mass are equal if the overbars refer to bulk average values. This method of following the reaction is, in principle, the same as the classic thermal method of measuring reactions in solution as described by Roughton and Chance (14).

EXPERIMENTAL

The primary object was to design a mixing device that would yield a concentration field effectively uniform on a coarse scale and nonhomogeneous over a long enough axial distance.

A number of mixing devices that had more or less known velocity fields were studied but none satisfied the required conditions. A satisfactory device was finally developed that consisted of 100, 0.052 in. I.D. parallel stainless steel tubes 4 or 5 in. long (Figure 1). These tubes were pressed into holes in a 1¼-in. diameter stainless steel disk that closed the upstream end of the 1¼-in. I.D. Lucite reactor. The tubes terminated at the disk. The reactant solutions were fed through alternate tubes. The Reynolds number was 3,700 in the tubes and 15,000 in the reactor. The bulk velocity of the jets leaving the disk was six times greater than the bulk velocity of 15.85 in./sec. in the reactor.

Deionized water was used to make up the reactant solutions. These solutions entered the reactor at 29.9°C. after passing through constant temperature baths.

The reaction was followed by a traversing 30 g. copper constantan glass shielded thermocouple probe whose reference junction was in one of the feed streams just before the mixing device. The effective tip diameter of the probe was 0.059 in. The probe was calibrated against a standard thermometer and also checked in the reactor using known heats of reaction.

The thermocouple signal was amplified by a Model-149 Keithley Millimicrovoltmeter and then electronically integrated. In general, temperature changes could be determined to within $\pm 0.005^\circ\text{C}$. A fine thermocouple probe (effective tip diameter of 0.015 in.) was also used to examine the jets in detail. Unless stated otherwise measurements were made with the large probe.

The signal from the probe at each station along the reactor was determined in the absence of reaction by passing pure water through the reactor. This signal was then subtracted from that obtained in the presence of reaction in order to correct for frictional heat generation, heat losses, and any small temperature difference between the two feed streams. The reactant feed concentrations were determined by repeated analyses during a run.

The systems used are given in Table 1. Since the temperature varied from 29.9 to 30.1°C. over the reactor, heats of reaction and other physical properties were taken at 30°C. The rate controlling steps are all second-order irreversible. Heats of reaction and reaction velocity constants are known. Most of the former and some of the latter could be measured directly in the reactor. In these cases the check with known values was good. However, the mechanism of the carbon dioxide-ammonia reaction is not known as well as the others, so the results with this system must be treated with caution. Details of the chemistry and thermodynamics are summarized elsewhere (18).

Temperature measurements taken over the cross section of the reactor at various downstream distances showed that the temperature profiles read by the large probe were almost flat (maximum difference in signal between any radial point and the mean was 4%, 3/16 of an inch from the inlet and less farther away). Thus, the centerline temperature was taken as a measure of the bulk temperature and this value was used

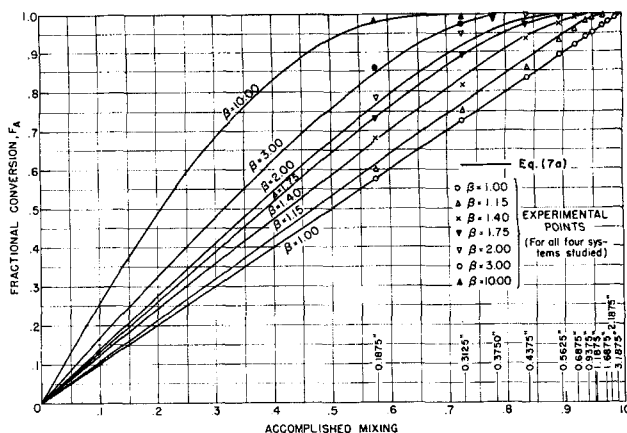


Fig. 3. Fractional conversion vs. accomplished mixing, very rapid reactions.

in Equation (10) to compute the conversion. Since the probe diameter is about the same as the initial jet diameters, the constancy of the temperature reading does not imply a uniform field.

VERY RAPID REACTIONS

The first four reactions in Table 1 are very rapid and serve as a test of the very rapid reaction theory. Nine separate experiments with stoichiometric mixtures of these reactants ($\beta = 1$) were carried out with inlet acid concentrations varying from 0.0139 g.-moles/l. to 0.0250 g.-moles/l. Inlet concentration of species i is defined as the moles of i entering the reactor per unit time divided by the total volumetric flow rate of both streams. From this point on, the subscript o refers to the inlet. This means that when (but only when) Equations (7) to (7c) are used the fluid is assumed to be uniform from the inlet on. Since β and n were 1 in all but the oxalic acid-lithium hydroxide reaction, where it was 2, the inlet base concentrations equalled the inlet acid concentrations in all but the latter reaction, where the inlet base concentration was twice the inlet acid concentration.

The fractional conversion vs. distance from the inlet disk is shown in Figure 2. The best value, as well as the upper and lower values, of all measurements at each Z are shown on the graph. The four different systems were indistinguishable, justifying the assumption of the very rapid theory that the molecular diffusivities of the two reactants may be treated as equal. The results are also in accord with the prediction that fractional conversion is independent of inlet concentration and stoichiometric ratio at a fixed β . The mean rate of reaction is of order 10^{-7} times the homogeneous mean rate. On the scale of

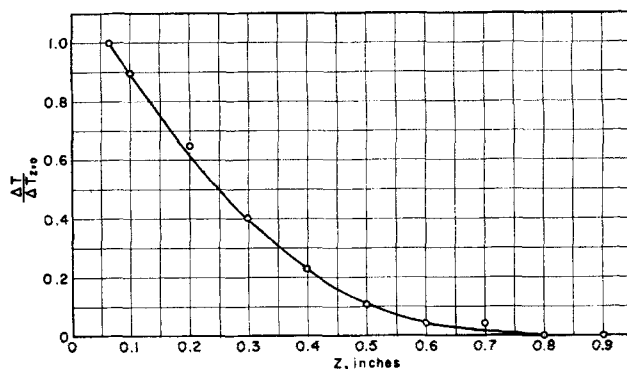


Fig. 4. Temperature differences between centers of hot and cold jets vs. distance.

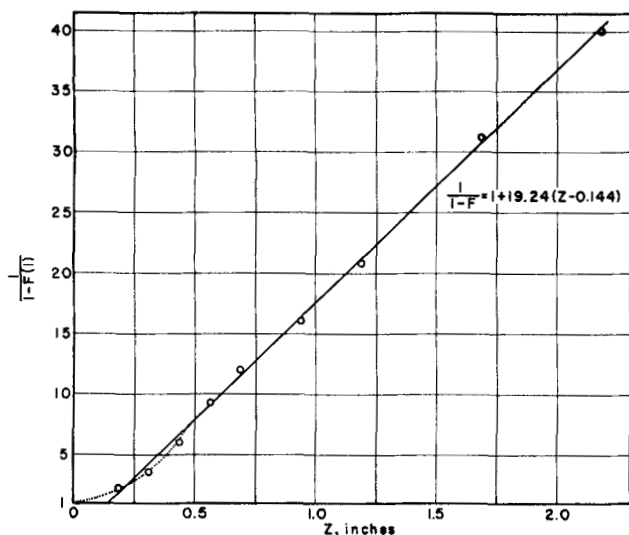


Fig. 5. Very rapid reactions, $\beta = 1$.

the graph the conversion predicted by the later rate law is a step function.

The RMS concentration fluctuation was not measured so Equation (7) cannot be checked directly as Keeler et al. did (8). However, a further check of the theory may be obtained by comparing the conversion measured at any β and Z to the conversion measured at the same Z with $\beta = 1$. The results are given in Figure 3. The solid lines are the predictions of Equation (7a). The $\beta = 1$ data were placed on the 45° line, Equation (7), and the data taken for $\beta > 1$ were located on the same abscissa as the $\beta = 1$ point taken at the same Z . This is equivalent to assuming Equation (7) to hold for $\beta = 1$ and using Equation (7a) to predict conversion of the limiting reactant for $\beta > 1$. The agreement is very good. Deviations between measured and predicted values are within experimental error. Again all four ionic reactions were used and were indistinguishable. $\beta = 1.4$ represents three separate runs, $\beta = 1.75$ five separate runs, and the other values of β single runs. Inlet concentrations of the limiting reactant covered the same range as those for $\beta = 1$. As predicted by Equations (7) and (7a), the conversion at a fixed β was independent of inlet concentration, n , and the choice of the limiting reactant.

It is important to note that agreement between theory and experiment has been obtained, even at the first station with β evaluated at the inlet concentrations [Equation (7c)]. Since Equations (7) and (7a) assume uniformity on a coarse scale, this indicates either that the concentration is effectively uniform very close to the inlet, or that the effect of β in a nonuniform field on the space mean concentration (or space mean reaction rate) is the same as in a uniform field.

In order to examine this unexpectedly good agreement so close to the inlet the fine thermocouple was used to probe the field. This was done by passing hot and cold water through alternate jets. The difference between the centerline temperatures of the hot and cold jets over the initial difference is plotted against distance in Figure 4. Although the jets are indistinguishable only after 0.8 in. (where the fractional conversion for $\beta = 1$ is 93%), much of the fluid is probably close to uniform at considerably shorter distances, since Figure 4 measures only the maximum nonuniformity. However, it does not seem likely that the fluid can be treated as uniform before the first station, 0.1875 in. Radial temperature measurements are being undertaken in order to investigate the extent of the nonuniformity.

When the data for $\beta = 1$ are plotted, as shown in Figure 5, a straight line results and by a least square calculation one finds

$$\frac{1}{1-F(1)} = 1 + 19.24 (Z - 0.144), Z > 0.144 \quad (11)$$

where Z is measured in inches. This is also the solid line of Figure 2. The excellent agreement between the equation and the mean of the measured values of F at each Z between 0.5 and 2.2 in. justifies the use of a linear relationship over this region, even though the uncertainty in $1/(1-F)$ naturally gets large as F approaches one.

The dotted line in both figures fits the data somewhat better when Z is less than about 0.5 in. and is a graph of the equation

$$1 - F(1) = e^{-0.295 Z} \quad (11a)$$

It intersects the solid line at $Z = 0.45$ in. This apparent change in the behavior suggests that the region of effective uniformity may begin around 0.45 in.

If Equation (11) is combined with Equation (7) then the unaccomplished mixing is given by the hyperbolic decay law

$$\frac{\Gamma_o}{\Gamma} = 1 + 19.24 (Z - 0.144), Z > 0.144 \quad (12)$$

while Equation (11a) gives an exponential decay. Note that Keeler et al. (8) and Gibson and Schwarz (6) obtained a decay law different from either of the above for flow behind a grid.

Equation (11) is of the same form as would be obtained for a homogeneous second-order chemical reaction with plug flow and no axial diffusion. [We really have no independent measures of the validity of the assumptions of plug flow and no axial diffusion. The effects do tend to cancel and estimates (unreliable) do indicate that deviations from the assumptions are small (18), but the main reason for their use is that they allow a simple description of the data.]

Thus, defining a mixing velocity constant, k_m , by

$$\bar{r}_A = -k_m \bar{C}_A \bar{C}_n \quad (13)$$

$$\frac{1}{1-F(1)} = 1 + k_m (1) n \bar{C}_A \frac{(Z - Z_1)}{u}, Z > Z_1 \quad (14)$$

where F has been taken as zero at $Z = Z_1$. Remember that \bar{C}_A is now the inlet concentration of A. The bulk

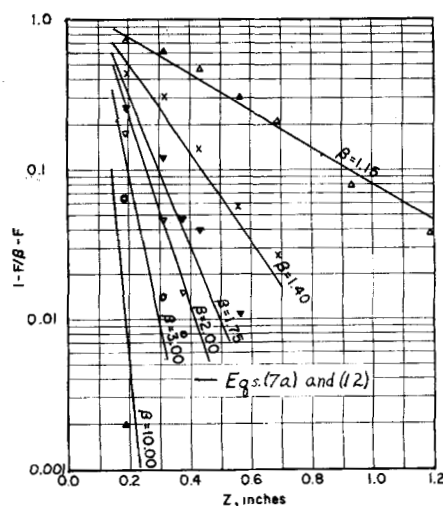


Fig. 6. Very rapid reactions.

average velocity in the reactor is 15.85 in./sec., hence from Equations (11) and (14)

$$k_m(1) = \frac{305}{n\bar{C}_{A_0} \text{ mole sec.}} \quad (15)$$

If Equation (11a) is used in place of (11) for $Z < 0.45$, then instead of a second-order rate law, one finds a first-order law for this region with a rate constant of 4.52 sec.⁻¹. Since the behavior at larger values of Z where the fluid is more uniform is of more immediate interest, the implications of the first-order law will not be pursued here.

The question immediately arises as to whether the second-order law, Equation (13), holds for β not equal to one. Using the stoichiometric relationship between \bar{C}_A and \bar{C}_B and integrating from $Z = Z_1$ where $F = 0$ one obtains

$$\ln \frac{1-F}{\beta-F} = -\ln \beta - (\beta-1) \frac{k_m n \bar{C}_{A_0}}{u} (Z - Z_1), \quad Z > Z_1 \quad (16)$$

If the experimental decay law, Equation (12), is combined with the very rapid reaction theory, Equation (7a), then the predicted conversion curves for $\beta \neq 1$ in Figure 3 are converted to conversion distance curves. These are indistinguishable from straight lines on the semilog graph of Figure 6 and hence to a very good approximation Equation (16) and hence Equation (13) is valid for $\beta \neq 1$ if Equation (13) holds for $\beta = 1$ (and the very rapid reaction theory is valid). The measured values for $\beta \neq 1$ are also shown on the graph. These are the same data as shown in Figure 3 but in this case the experimental values are compared to Equation (7a) using Equation (12) or (11) rather than the raw $\beta = 1$ data as was done in Figure 3.

The fit is better for the smaller values of Z if Equation (11a) is used in place of Equation (11) so the data for $\beta \neq 1$ also indicate the Equation (11a) fits the $\beta = 1$ data better than Equation (11) for small Z . We conclude then that the very rapid reaction data fit a second-order rate law better as the fluid becomes more uniform.

By taking slopes of the theoretical lines in Figure 6 one obtains

$$k_m = \frac{305}{n \bar{C}_{A_0}} g(\beta) \quad (15a)$$

where $g(\beta)$ varies from one at $\beta = 1$ to 0.30 at $\beta = 10$.

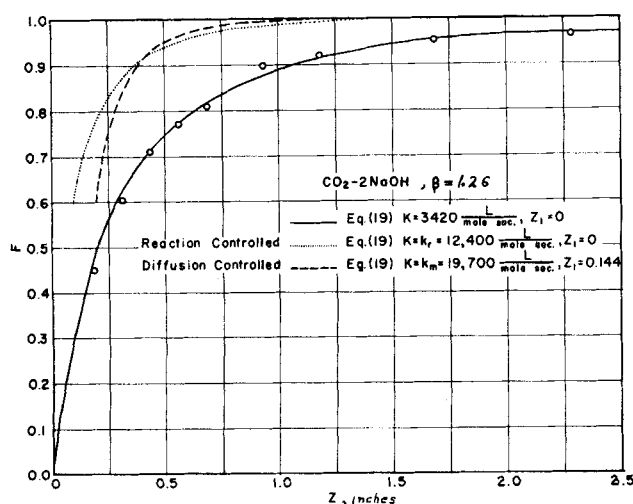


Fig. 7. F vs. Z , rapid reaction, $\text{CO}_2\text{-2NaOH}$, $\beta = 1.26$.

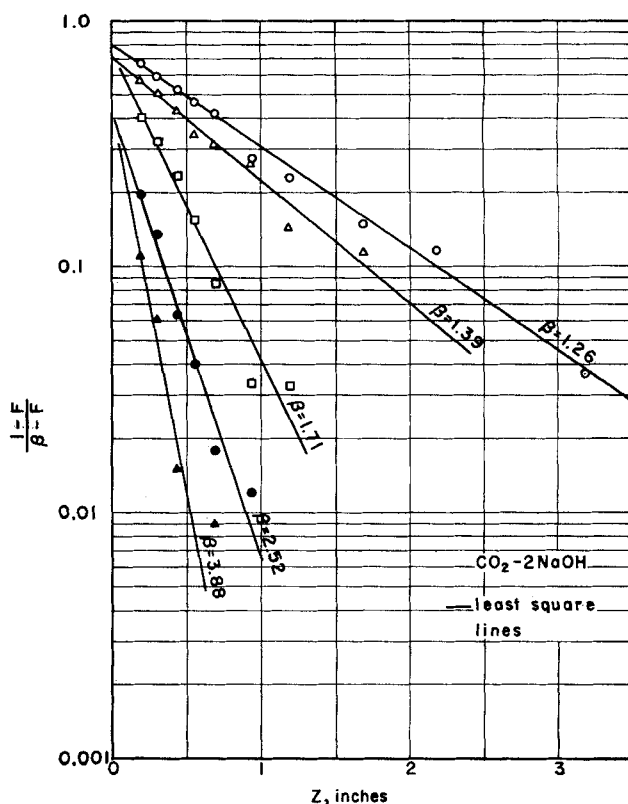


Fig. 8. Rapid reaction, $\text{CO}_2\text{-2NaOH}$.

Since the form of the decay law depends upon the mixing device, the second-order behavior must be treated as a peculiarity of the device. Nevertheless the behavior may be used to set up a useful criterion for relative reaction rates in this device.

Thus if the reaction mixing (R.M.) number

$$N_{RM} = \frac{k_r}{k_m} = \frac{n\bar{C}_{A_0} k_r}{305 g(\beta)} \quad (17)$$

is much greater than one the reaction is very rapid; if much less than one, it is slow and if order one is rapid. Note that the criterion depends upon inlet concentration as well as upon mixing rate and reaction velocity.

Since k_m is in the range of 10,000 to 20,000 l./mole sec., this criterion properly implies that ionic reactions ($N_{RM} \approx 10^7$) are very rapid.

The mean rate of a very rapid reaction has been shown to be independent of the chemical reaction velocity constant since the reaction is diffusion controlled. As k_r is decreased it would be expected that the effect of k_r would become important as the R.M. number approaches one and become controlling as the number gets much less than one.

The carbon dioxide-sodium hydroxide system has an R.M. number in the range of 0.5 to 1.0 for the concentration ranges available in this work. Typical F - Z data are given in Figure 7 and data for all runs in Figure 8. F is the conversion of the limiting reactant, carbon dioxide, whose inlet concentration was close to 0.007 moles/l. in all runs. The data of Figure 8 are fitted closely by straight lines. The least square lines shown intersect $F = 0$ between $Z = 0$ and 0.05 in. and there is no significant deviation at the small values of Z as occurred with very rapid reactions. Hence the second-order rate law

$$\bar{r} = -K \bar{C}_A \bar{C}_B \quad (18)$$

TABLE 2. RAPID REACTIONS

CO ₂ -2NaOH						
β	k_r , 1.	k_m , 1.	N_{rm}	K , mole sec.	$-\frac{C_A' C_B'}{\bar{C}_A \bar{C}_B}$	K (Eq. 22), 1.
1.26	12,400	19,700	0.63	3420	0.72	7610
1.39		21,200	0.59	3750	0.70	7820
1.71		17,700	0.70	4780	0.61	7290
2.52		15,300	0.81	3260	0.74	6850
3.88		9,400	1.30	2770	0.78	5350
CO ₂ -nNH ₃						
2.1	585	24,500	0.024	588	0.0	571
2.3		23,300	0.025	519	0.11	571
3.6		18,400	0.032	550	0.06	567
4.6		12,400	0.047	454	0.22	559
5.75		12,300	0.048	336	0.43	558

with plug flow and no axial mixing applies since the integrated form

$$\ln \frac{1-F}{\beta-F} = -\ln \beta - \frac{K(\beta-1)n\bar{C}_{A_0}(Z-Z_1)}{u} \quad (19)$$

gives the straight lines of Figure 8. The values of K , the apparent reaction velocity constant, were determined from the slope of these lines and are given in Table 2.

Equation (19) with the least square slope is shown as the solid line in Figure 7 and the other lines represent the two limiting conversion curves. The dotted line is the conversion which would be obtained if the fluid were homogeneous throughout, $K = k_r$, $Z_1 = 0$, (it will be seen that this corresponds to a small R.M. number) and the dashed line the conversion which would be obtained if the reaction were very rapid, $K = k_m$, $Z_1 = 0.144$. The measured conversion is less than either of these limiting values, K is less than either k_m or k_r . K is compared to these values in Table 2 for all runs.

The carbon dioxide-ammonia system has an R.M. number of order 10^{-2} . The data are shown in Figure 9 and the values of K computed from the least square lines shown are given in Table 2. The intersect of the lines with $F = 0$ occurs at a value of Z between -0.1 and $+0.1$ in. The data show some curvature which may be due to side reactions. The reaction mechanism in this system is uncertain (18) so these results are not too reliable.

SLOW REACTIONS

The reaction methyl formate-sodium hydroxide has an R.M. number of the order 10^{-3} . The data are given in Figure 10 and are compared to the normal homogeneous rate law [mean rate equals homogeneous mean rate, Equation (19) with $K = k_r = 47$ l./mole sec. and $Z_1 = 0$]. Agreement is very good out as far as 15 in., but only the first 3 in. are shown. The data fit the homogeneous rate law right through the nonuniform region.

DISCUSSION

Contrary to one's first guess, one does not find a non-homogeneous region where the reaction is slowed down by the unmixedness followed by a homogeneous region in which the reaction proceeds at the homogeneous mean rate. Rather, it is found that throughout this reactor (after a short initial distance and to as great a distance as can be measured) the mean rate in any one run is a fixed fraction, K/k_r , of the homogeneous mean rate, even

though the fluid is becoming more homogeneous as Z increases, and this fraction depends upon the R.M. number. As the R.M. number decreases from a very large value the fraction increases from a very small number ($\sim 10^{-7}$) to one as the R.M. number approaches zero. Thus for a given nonhomogeneity, that is, at a given Z , the fractional decrease in the mean rate of reaction from the homogeneous mean rate due to the unmixedness decreases as the R.M. number goes to zero. This accounts for the shift of the intersect of the second order rate law towards zero as the R.M. number decreases. (Compare Figures 5 and 6 with Figures 8, 9, and 10.)

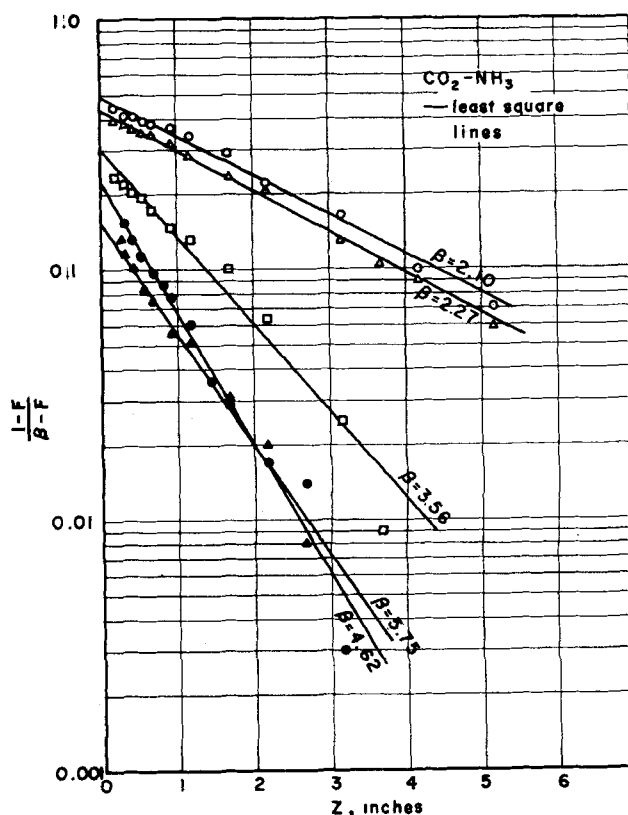
The methyl formate-sodium hydroxide reaction fits the homogeneous mean second-order rate law right from $Z = 0$, so the decrease in the mean rate caused by the unmixedness is apparently below the measurable level at this low value of the R.M. number. However a small decrease may be obscured by the assumptions of plug flow and no axial diffusion.

The orders of magnitude of the R.M. ratios studied are

$$10^7, 10^6, 10^{-2}, 10^{-3}$$

at 10^7 the reaction is diffusion controlled, $K = k_m$; at 10^{-3} it is reaction controlled, $K = k_r$; while the two intermediate cases are influenced by both mechanisms (Table 2). In the intermediate cases the mean rate of reaction is always less than the homogeneous mean rate and the diffusion controlled rate, K is less than either k_r or k_m .

On a fine scale the local instantaneous rate of reaction is a hydrodynamically complicated problem of simultaneous diffusion and reaction. Although the problem is a difficult one to analyze in detail, an analysis of the features of the instantaneous concentration profiles shows that in a nonhomogeneous mixture the mean rate must be less than the homogeneous mean rate and in a mixture in which the R.M. number is not large the mean rate must also be less than the diffusion controlled rate.

Fig. 9. Rapid reaction, CO₂-NH₃.

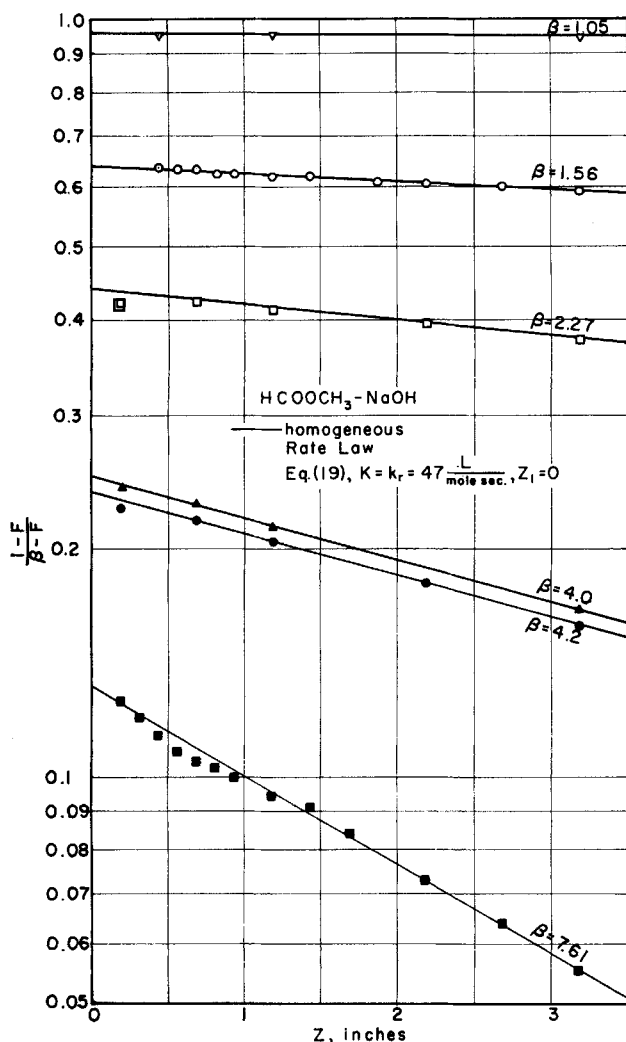


Fig. 10. Slow reaction, $\text{HCOOCH}_3\text{-NaOH}$.

Equation (5) gives another viewpoint— $\overline{C_A' C_B'}$ must be negative; hence the mean rate must be less than the homogeneous mean rate in a nonhomogeneous mixture as was pointed out earlier.

$\overline{C_A' C_B'}$ is now known if the assumptions of plug flow and negligible axial diffusion are valid, since from Equations (5) and (18)

$$-\frac{\overline{C_A' C_B'}}{\overline{C_A C_B}} = 1 - \frac{K}{k_r} \quad (20)$$

Values are given in Table 2. When the second-order rate law holds $\overline{C_A' C_B'}/\overline{C_A C_B}$ is independent of distance. $\overline{C_A' C_B'}$ depends upon both the diffusion and the reaction. The quantity decays with distance whatever the R.M. number, but the rate of decay depends upon the R.M. number.

Since the diffusion and reaction steps are coupled one does not expect simple relationships among K , k_r , and k_m for rapid reactions. One approach to this problem is to note that for very rapid reactions $\overline{C_A' C_B'} = -\overline{C_A C_B}$; hence Equation (18) can be written as

$$\overline{r} = k_m \overline{C_A' C_B'} \quad (21)$$

If this relationship is assumed to describe the *mixing step* even when the reaction is not very rapid, then combination with Equations (5) and (18) gives

$$\frac{1}{K} = \frac{1}{k_r} + \frac{1}{k_m} \quad (22)$$

This equation correctly handles the very rapid and slow reactions, but tends to give too high a value for the rapid reactions (Table 2); it may be looked upon as a rough interpolation rule.

ACKNOWLEDGMENT

The authors are grateful to the National Science Foundation for the financial support of this work and to Dr. C. V. Seshadri for the temperature measurements shown in Figure 4.

NOTATION

- A, B = species A, B
- C_i = molar concentration of species i
- C_i' = fluctuating component of C_i
- C_p = heat capacity of solution
- D = molecular diffusivity of mass
- F = fractional conversion based on average concentrations
- $F(1)$ = F at $\beta = 1$
- $g(\beta)$ = defined by Equation (15a)
- ΔH = heat evolved per mole of A reacted
- ierfc = first integral of complementary error function
- K = apparent reaction velocity constant defined by Equation (18)
- k_m = mixing velocity constant, limit of K for very rapid reactions
- $k_m(1)$ = k_m at $\beta = 1$
- k_r = reaction velocity constant
- n = stoichiometric coefficient
- N_{RM} = reaction mixing number
- r = reaction rate
- T = temperature
- \bar{u} = bulk average velocity in reactor
- V = velocity vector
- V' = fluctuating component of V
- Z = axial distance measured from reactor inlet
- Z_1 = value of Z at which F is zero

Greek Letters

- α = molecular diffusivity of heat
- β = $\overline{C_{Bo}}/n\overline{C_{Ao}}$
- Γ^o = $\sqrt{\overline{C_o'^2}}$
- Γ_o^o = $\sqrt{\overline{C_o'^2}}$
- γ_o = defined by Equation (7b)
- ϵ = eddy diffusivity of mass
- ϵ_z = eddy diffusivity of mass in Z direction
- ϵ_{hz} = eddy diffusivity of heat in Z direction
- θ = time
- ρ = density of solution

Subscripts

- i = species A or B
- o = inlet to reactor or position at which uniformity begins

Superscripts

- o = mixing without reaction
- = time or bulk average value

LITERATURE CITED

1. Burke, S. P., and T. E. W. Schumann, *Ind. Eng. Chem.*, **20**, 998 (1928).
2. Corrsin, S., *J. Fluid Mech.*, **11**, Pt. 3, 407 (1961).
3. —, *Phys. Fluids*, **1**, 42 (1958).
4. —, *ibid.*, **7**, 1156 (1964).
5. Eyring, H., and E. M. Eyring, "Modern Chemical Kinetics," Reinhold, New York (1963).
6. Gibson, C. H., and W. H. Schwarz, *J. Fluid Mech.*, **16**, Pt. 3, 365 (1963).

7. Hawthorne, W. R., D. S. Weddell, and H. C. Hottel, "Third Symp. Combustion and Flame and Explosion Phenomena," p. 266, Williams and Wilkins, Baltimore, Md. (1949).
8. Keeler, R. N., E. E. Petersen, and J. M. Prausnitz, *A.I.Ch.E.J.*, **11**, No. 2, 221 (1965).
9. Kramers, H., Jr., *Intern. Ser. Monographs Chem. Engr.*, **1**, 45 (1957).
10. Kristmanson, D., and P. V. Danckwerts, *Chem. Eng. Sci.*, **16**, 267 (1961).
11. Leimu, R., R. Korle, E. Laaksonen, and V. Lehmuskoski, *Suomen Kemistilehti*, **19B**, 93 (1946).
12. Pinsent, B. R. W., L. Pearson, and F. J. W. Roughton, *Trans. Faraday Soc. (London)*, **52**, 1512 (1956).
13. ———, *ibid.*, 1594 (1956).
14. Roughton, F. J. W., and Britton Chance, "Technique of Organic Chemistry," S. L. Friess, E. S. Lewis, A. Weissberger, Eds., Vol. VII, Pt. II, p. 703, Interscience, New York (1963).
15. Toor, H. L., *A.I.Ch.E. J.*, **8**, 70 (1962).
16. Van Krevelen, D. W., and C. J. Van Hooren, *Rec. Trav. Chim.*, **67**, 587 (1948).
17. ———, P. J. Hoftijzer, and F. J. Huntjens, *ibid.*, **68**, 191 (1949).
18. Vassilatos, G., Ph.D. thesis, Carnegie Inst. Technol., Pittsburgh, Pennsylvania (1964).

Manuscript received October 10, 1964; revision received February 15, 1965; paper accepted February 17, 1965. Paper presented at A.I.Ch.E. Boston meeting.

A Pitot Tube Method for Measuring the First Normal Stress Difference and Its Influence on Laminar Velocity Profile Determinations

J. G. SAVINS

Socony Mobil Oil Company, Inc., Dallas, Texas

A scheme is outlined which enables the calculation of the normal stress difference $P_{11}-P_{22}$ in fluids undergoing steady Poiseuille flow from measurements with a pitot tube of local velocity distributions. This new technique should enable measurements in a region of shear rate comparable to that encountered in the torsional and circular flow methods. A particularly interesting consequence of the method is it leads one to the inescapable conclusion that the presence of finite normal stresses should produce significant aberrations on the measurement of the velocity profile in the laminar flow of viscoelastic fluids. The presence of a $P_{11}-P_{22}$ induced aberration on the velocity profile measurement suggests that caution be exercised in the practice of deducing estimates of the thickness of a boundary layer in the nonlaminar flow of these fluids.

Considerable effort is being given by experimental rheologists to the problem of developing tools for the quantitative measurement of normal stresses in viscoelastic fluids. Although there does not appear to be a universally preferred technique, the various methods currently used can be sharply divided into two main categories: providing data primarily for the purpose of evaluating constitutive equations and measuring properties under those conditions which a fluid of interest will encounter in flow through actual process equipment. The torsional (1 to 8) and circular flow techniques (1 to 4, 9 to 11) are typical of the first category. The jet expansion and thrust methods (2, 4, 7, 12 to 16) illustrate the second category. With the application of appropriate assumptions, either method yields a reasonable description of the normal stresses as a function of shear rate. It is unfortunate, however, that the jet/thrust methods which have their origins in the viscometric flow familiar to rheologists as Poiseuille flow or tube viscometer flow are, for a variety of reasons, usually restricted to measurements of normal stresses at

shear rates not less than 10^8 sec^{-1} , whereas the torsional and circular flow methods seldom approach shear rates as high as 10^8 sec^{-1} . Thus one is faced with the problem of extrapolating results over a decade or more of shear rate in order to compare results from different experimental techniques. Because the Poiseuille flow case is representative of the class of exactly solvable viscometer flows,* it would be desirable to be able to measure the normal stress under conditions of shear rate comparable to those encountered in the first category of methods.

The purpose of this paper is to outline a scheme for experimentally determining the first normal stress difference $(P_{11} - P_{22})^\dagger$ at low shear rates from measurements of point values of dynamic pressures with a pitot tube under the steady laminar conditions of Poiseuille flow. A particularly interesting consequence of the proposed

* The torsional and circular flow methods represent a class of problems which are not compatible with the dynamical equations unless inertia is neglected.

† In the language of Coleman and Noll (17), the material function difference $\sigma_2(\Gamma_R) - \sigma_1(\Gamma_R)$.